JACS
JOURNAL OF THE AMERICAN CHEMICAL SOCIETY
pubs.acs.org/JACS
Article

Cytosine Methylation Enhances DNA Condensation Revealed by Equilibrium Measurements Using Magnetic Tweezers

Ya-Jun Yang, Hai-Long Dong, Xiao-Wei Qiang, Hang Fu, Er-Chi Zhou, Chen Zhang, Lei Yin, Xue-Feng Chen, Fu-Chao Jia, Liang Dai, Zhi-Jie Tan, and Xing-Hua Zhang*

Cite This: *J. Am. Chem. Soc.* 2020, 142, 9203−9209

ABSTRACT: CpG methylation of DNA is common in mammalian cells. In sperm, the DNA has the highest level of CpG methylation and is condensed into toroidal structures. How CpG methylation affects DNA structures and interactions is important to understand its biological roles but is largely unknown. Using an RNA−DNA−RNA structure, we observed the equilibrium hopping dynamics between the condensed and extended states of DNA in the presence of polyamines or polylysine peptide as a reduced model of histone tails. Combing with the measured DNA elasticities, we report that CpG methylation of each cytosine nucleotide substantially increases DNA−DNA attraction by up to 0.2 k_BT. For the DNA with 57% GC content, the relative increase caused by CpG methylation is up to 32% for the spermine-induced DNA−DNA attraction and up to 9% for the polylysine-induced DNA−DNA attraction. These findings help us to evaluate the energetic contributions of CpG methylation in sperm development and chromatin regulation.

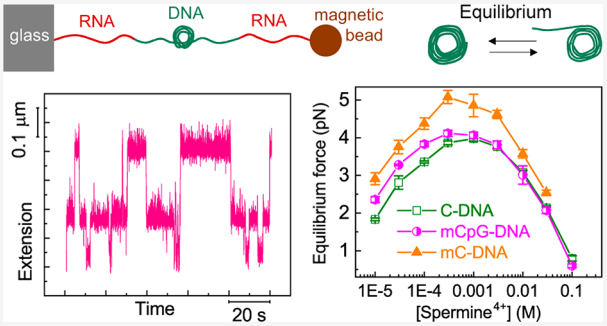

■ INTRODUCTION

Despite strong repulsion between negatively charged backbones, DNA can be condensed by many cationic counterions, such as high-valent ($N \geq 3$) cations, cationic surfactants, lysine/arginine-rich peptides, and cationic proteins.[1,2] DNA condensation and decondensation are properly regulated in cells to facilitate DNA packing, DNA replication, and gene transcription. How to effectively control DNA condensation is very important in many biological processes and can be useful in applications, such as gene delivery. DNA condensation should depend on not only the external conditions of DNA molecules but also the chemical modification to DNA. Methylation is arguably the most important chemical modification to DNA. How methylation affects DNA condensation, however, remains largely unclear.

In mammals, most DNA methylation occurs at cytosine nucleotides at CpG (a cytosine nucleotide followed by a guanine nucleotide) sites. The CpG methylation is tied strongly to cell development, pluripotency, carcinogenesis, transcriptional regulation, chromatin remodeling, aging, cancer, etc.[3−6] The level of CpG methylation is the highest in sperm where DNA is condensed into close-packed toroidal subunits.[4] In somatic cells, the DNA has well-regulated CpG methylation and is packed into nucleosomes, then further packed into chromosomes. Thus, it is of great interest to know whether methylation plays a role in DNA condensation.

Single-molecule techniques have been demonstrated to be effective tools to study the mechanism and kinetics of DNA condensation as well as the elasticities of DNA in the presence of condensing agents.[7−18] Recently, single-molecule fluorescence experiments and molecular dynamics simulations have revealed that the methyl groups could relocate the high-valent cations from major grooves of DNA to interhelical regions, thereby increasing DNA−DNA attraction.[19,20] In this work, to quantify the effects of CpG methylation, we will study the condensation of methylated DNA at equilibrium in the presence of high-valent cations using single-molecule magnetic tweezers. Combing with the measured elasticities of DNA before condensation, we will calculate the change in DNA−DNA attraction that drives DNA condensation caused by CpG methylation. These results will help us to evaluate how CpG methylation affects the development of sperm and the regulation of chromatin dynamics.

■ MATERIALS AND METHODS

We tethered a single DNA between an antidigoxigenin coated coverglass and a streptavidin-coated superparamagnetic bead (Figure 1a). After bead tethering, we passivated the glass and bead surfaces using 10% w/v MPEG-Succinimidyl Valerate ester (MW 2K, Hunan

Received: November 5, 2019
Published: April 24, 2020

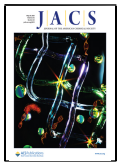

https://dx.doi.org/10.1021/jacs.9b11957
J. Am. Chem. Soc. 2020, 142, 9203−9209

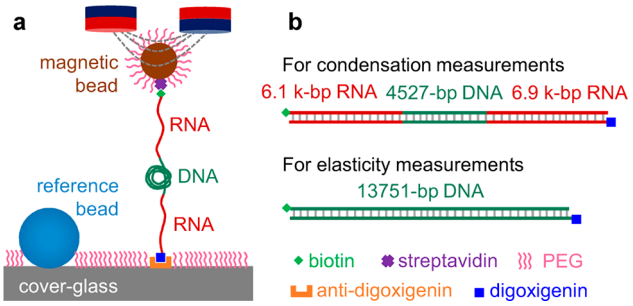

Figure 1. Experimental setup. (a) Home-built magnetic tweezers. (b) DNA constructs for condensation and elasticity measurements.

Huateng Pharmaceutical) for 2 h. We acquired all data at 10 mM Tris-HCl pH 7.5 and 22 °C. See more details of the home-built magnetic tweezers in our previous works.[21−27]

Taking advantage of double-stranded (ds) RNA that resists condensation,[28] we used two long dsRNA handles to protect the inside 4527 bp dsDNA from possible interactions with the substrate surfaces in DNA condensation experiments (Figure 1b). In DNA elasticity measurements, we used a 13751 bp long dsDNA to achieve high precision. The nonmethylated DNA (C-DNA) was amplified through ordinary PCR using KOD-plus DNA polymerase (TOYO-BO). We added methyl groups to the cytosine nucleotides at CpG sites (mCpG-DNA) using CpG Methyltransferase (New England Biolabs). To magnify the effects of cytosine methylation for detection, we added methyl groups to all cytosine nucleotides (mC-DNA) through PCR using 5-methyl-dCTP (New England Biolabs). Please find the protocols to prepare the DNA constructs in the Supporting Information (Figure S1a,b) and our previous work.[23] The 4527 bp DNA contains 2575 cytosine nucleotides, out of which 828 are located at CpG sites. The 13751 bp DNA contains 7865 cytosine nucleotides, out of which 1166 are located at CpG sites. The efficiency of cytosine methylation was confirmed using BstUI (New England Biolabs) whose cleavage ability was blocked by CpG methylation (Figure S1c,d).

We purchased Hexammine cobalt(III) chloride ($CoHex^{3+}$), Spermidine·3HCl ($Spermidine^{3+}$), and Spermine·4HCl ($Spermine^{4+}$) from Sigma-Aldrich. These high-valent cations were widely used to study DNA condensation and DNA−DNA interactions.[13−20,29−32] We synthesized the polylysine peptide Hexa-lysine·6HCl (PLL^{6+}) in Sangon Biotech as a reduced model of the highly charged, intrinsically disordered, lysine-rich histone tails.[20]

To determine the nucleation (F_n) and equilibrium (F_e) condensation forces, we stretched the RNA−DNA−RNA molecule by repeating force-cycles in the presence of high-valent cations. Each cycle contained four force regions (Figure 2a): (i) A force-decreasing region where the applied force was successively kept at a series of constant forces reduced at −0.01 pN/s and during force-decreasing the DNA nucleated and condensed; (ii) A region where a low constant force was kept for 20 s; (iii) A force-increasing region where the applied force was successively kept at a series of constant forces raised at 0.01 pN/s and during force-increasing the DNA passed by the equilibrium point and then completely decondensed at even high forces; (iv) A region where a high constant force was kept for 10 s. In the force-decreasing region, the reduction in extension during condensation was always slightly shorter than the extension of 4527 bp DNA, indicating the RNA handles did not condense. In the force-increasing region and force-decreasing region, we calculated the average and variance of the extension at each constant force (Figure 2b). We determined F_n and F_e by an abrupt increase in the variance of molecule extension.[24−26]

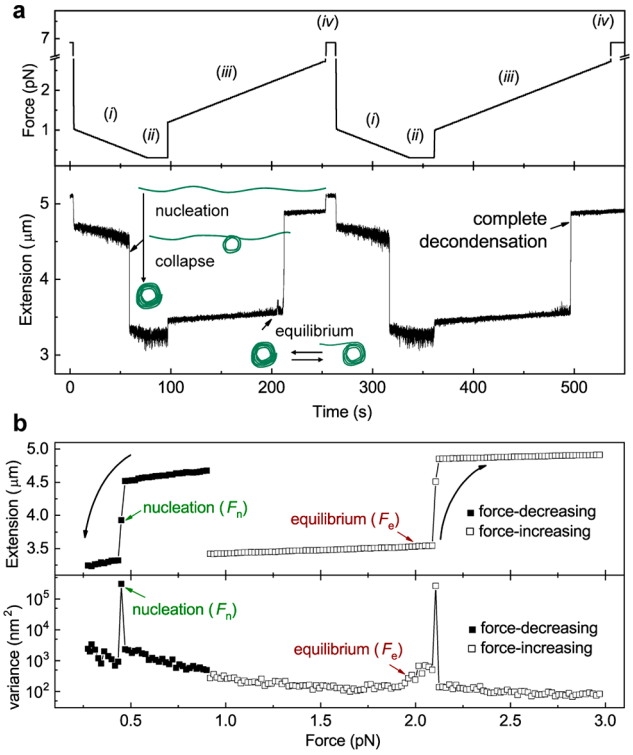

Figure 2. Determining the condensation forces by repeating force-cycles. The representative curves were obtained at 0.2 mM $CoHex^{3+}$ using C-DNA. (a) The time-extension course recorded during repeating force-cycles. (b) The nucleation (F_n) and equilibrium (F_e) condensation forces marked by the abrupt increase in the variance of molecule extension.

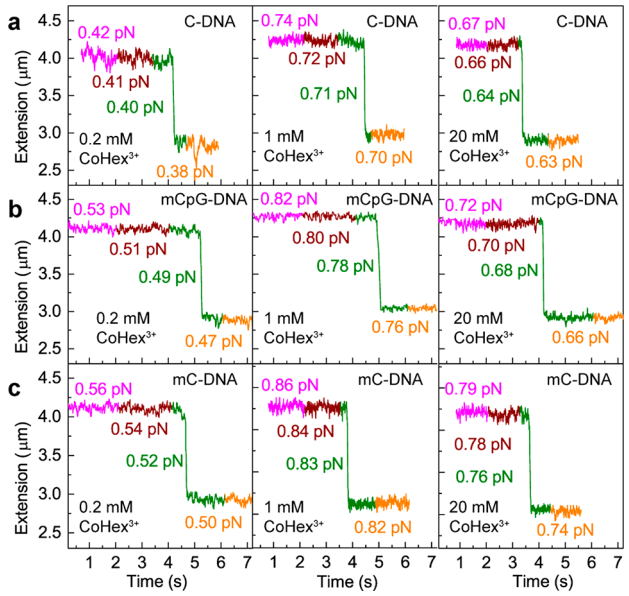

Figure 3. One-step kinetics from the extended state to the condensed state of DNA during force-decreasing.

RESULTS

The Kinetics of DNA Condensation under Tension. Whether methylated or not, the DNA condensed in a one-step manner in the force-decreasing region (Figure 3), which can be explained by the nucleation-collapse mechanism.[15,16] To overcome the large energy barriers, the nucleation occurred at forces much lower than the energy equilibrium. Immediately after nucleation, the DNA rapidly condensed against the low nucleation force.

https://dx.doi.org/10.1021/jacs.9b11957
J. Am. Chem. Soc. 2020, 142, 9203−9209

After DNA condensation, we stretched the condensed DNA through a serious of increasing constant forces near the equilibrium (Figure 2). To detect the kinetics more clearly, we held each constant force for hundreds of seconds (Figure 4).

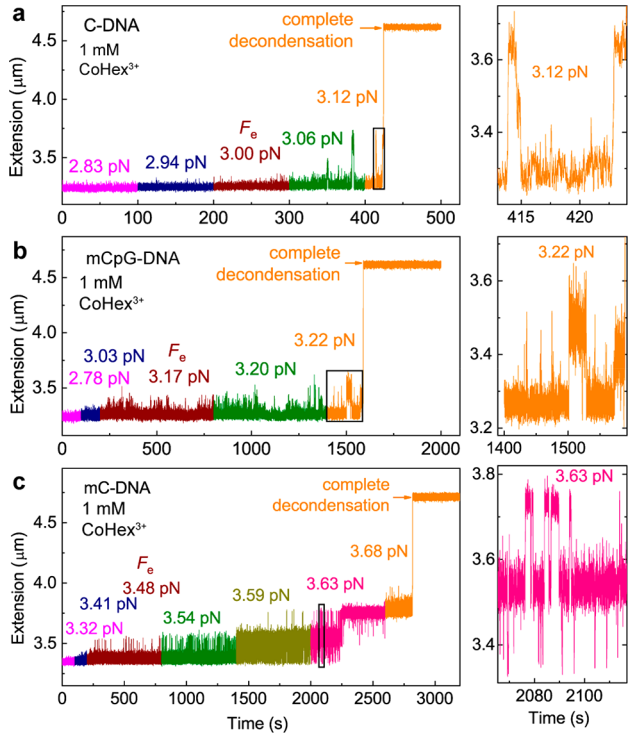

Figure 4. The hopping kinetics between the extended and condensed states of DNA at constant forces. The detailed time-courses in the black rectangles were magnified for clarity.

For all of the C-DNA, mCpG-DNA, and mC-DNA, we observed the hopping kinetics of DNA extension near the equilibrium at constant forces (magnified panels), which indicates the coexistence of the extended and condensed state of DNA. Forces of about 0.2 pN higher than F_e (wine) led to complete decondensation of the DNA.

Cytosine Methylation Enhances DNA Condensation. With the increase in the concentration of $CoHex^{3+}$, $Spermidine^{3+}$, or $Spermine^{4+}$, both F_n and F_e first increase and then decrease (Figure 5). The reverse of trend is probably due to the charge-inversion of DNA caused by the excessive binding of high-valent cations.[15,16] The peak values of F_n and F_e increase with the valence of cations (PLL^{6+} > $Spermine^{4+}$ > $CoHex^{3+}$ > $Spermidine^{3+}$). We only measured until 0.1 mM PLL^{6+} as dsRNA handles might condense or interact with the glass/bead surfaces at higher PLL^{6+} concentrations (Figure S2). Such RNA condensation or RNA-surface interaction may disturb the measurement of DNA condensation.

Figure 5 compares DNA condensation for DNA samples with three levels of cytosine methylation: C-DNA, mCpG-DNA, and mC-DNA. For all the four cations, cytosine methylation enhances DNA condensation as indicated by the increases in F_n and F_e. In Figure 5, we used the loading/unloading rates of ±0.01 pN/s. To determine the effects of loading/unloading rates, we further measured F_n and F_e at ±0.001 and ±0.003 pN/s in the presence of 5 mM $CoHex^{3+}$ (Figure S3). We found F_n slightly increased at low rates whereas F_e kept constant, which were consistent with the

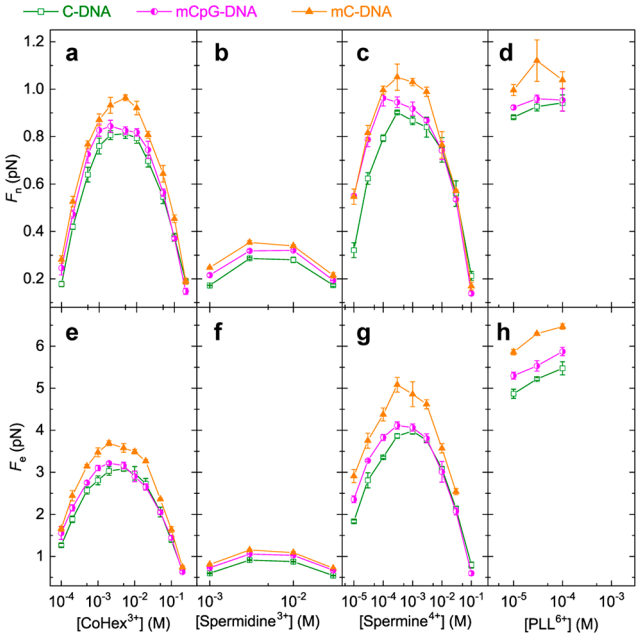

Figure 5. Effects of cytosine methylation on the nucleation and equilibrium condensation forces. At each cation condition, the averages and standard errors of F_n and F_e obtained from more than three molecules were plotted as data points and error bars. We only measured until 0.1 mM PLL^{+6} to avoid RNA condensation.

nonequilibrium nature of F_n and the equilibrium nature of F_e. The rate-independent F_e will be used to quantify the enhancement of DNA−DNA attraction caused by cytosine methylation.

DNA Elasticities in the Presence of High-Valent Cations. To obtain the changes in DNA extension during DNA condensation, we next determined DNA elasticities in the presence of high-valent cations using the 13751 bp DNA. To avoid DNA condensation and DNA−surface interactions, we only measured the force−extension curves of DNA at higher forces (Figure S4). We fitted each force−extension curve to the extensible worm-like chain model:[33]

$$\frac{x}{NL} = 1 - \sqrt{\frac{k_B T}{4FP}} + \frac{F}{K} \quad (1)$$

Here, N is the number of base pairs of the DNA. The measured variables x is the DNA extension and F is the applied force. The fitting parameters L is the contour length per base pair, P is the bending persistence length, and K is the stretching modulus.

Figure 6 shows that in the cases of $CoHex^{3+}$, $Spermidine^{3+}$, and $Spermine^{4+}$, P, L, and K decrease first and then increase with the increase in cation concentrations. The reverse of the trend may be attributed to charge-inversion of DNA caused by excessive binding of high-valent cations.[16,27] In the case of PLL^{6+}, both P and L decrease and then reach plateaus, while K keeps increasing. We did not further increase the concentration of PLL^{6+} to avoid DNA−surface interactions.

The enhancement of the bending flexibility of an isolated DNA will be critical especially in nanoscale bending of DNA fragments, a prerequisite process of DNA condensation.[1,12] The shortening of DNA contour length means the same spatial length of DNA contains more DNA base pairs (i.e., more charge interactions between DNA base pairs). Thus, high-valent cations soften and shorten DNA, and both of the effects

https://dx.doi.org/10.1021/jacs.9b11957
J. Am. Chem. Soc. 2020, 142, 9203−9209

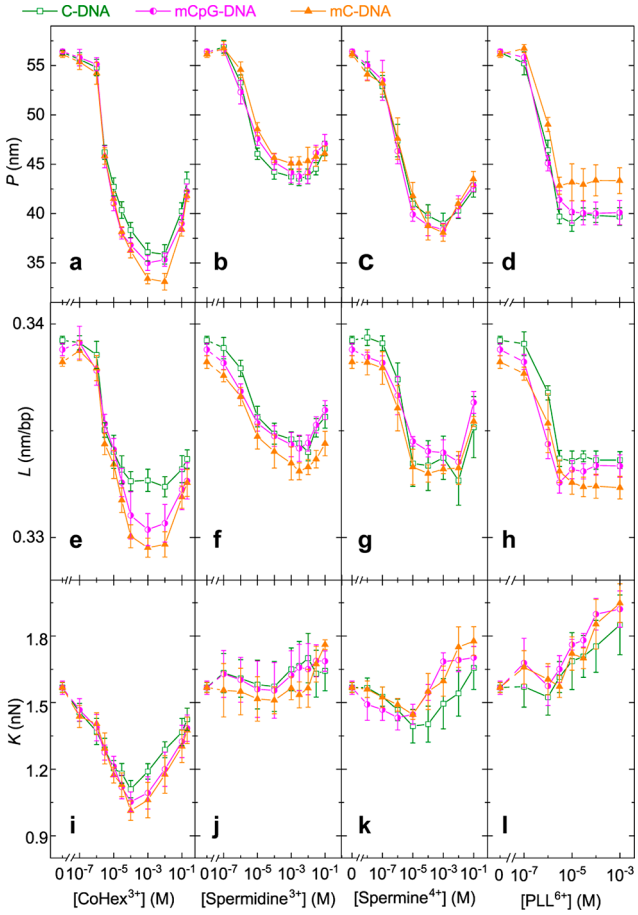

Figure 6. The elasticities of DNA in the presence of high-valent cations. At each cation condition, the average and standard error of bending persistence length (P), contour length per base pair (L), and stretching modulus (K) obtained from more than three molecules were plotted as data points and their error bars.

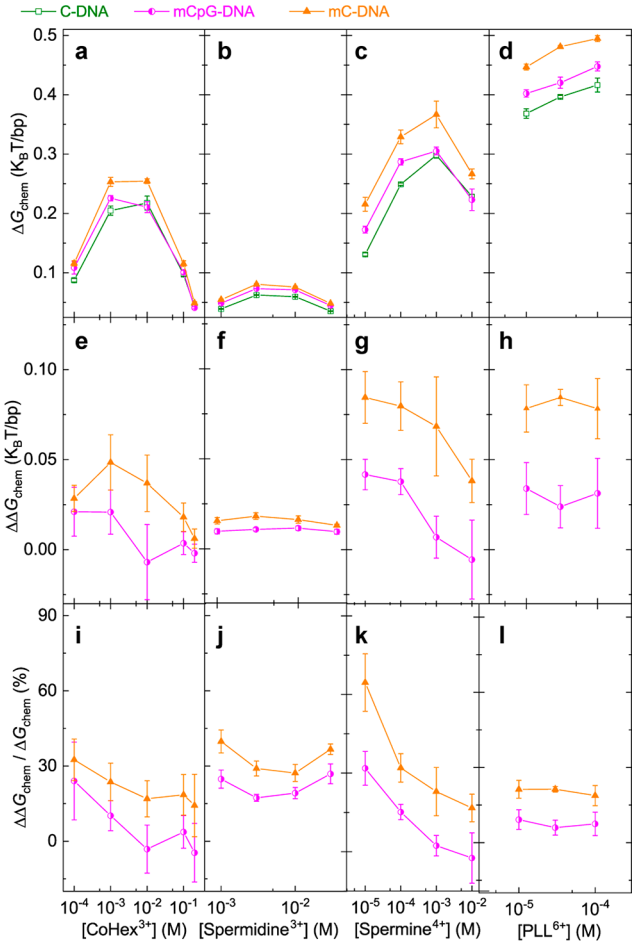

Figure 7. Cytosine methylation increases DNA−DNA attraction. At each cation condition, the average and standard error of DNA−DNA attraction calculated from more than three molecules were plotted as a data point and its error bar. (a−d) The DNA−DNA attraction per base pair without external force (ΔG_{chem}) for C-DNA, mCpG-DNA, and mC-DNA. (e−h) The change in ΔG_{chem} caused by cytosine methylation. (i−l) The percentage change in ΔG_{chem} caused by cytosine methylation.

benefit DNA condensation. Figure 6 shows that cytosine methylation slightly softens and shortens DNA in the presence of $CoHex^{3+}$, but not in the presence of $Spermine^{4+}$, $Spermidine^{3+}$, or PLL^{6+}.

Quantifying the Enhancement of DNA−DNA Attraction Caused by Cytosine Methylation. On the basis of the measured equilibrium DNA condensation force (Figure 5e−h) and DNA elasticities (Figure 6), we calculated the DNA−DNA attraction that drives DNA condensation. At the equilibrium, the extended and condensed DNA states coexist, which gives

$$\Delta G = \Delta G_{chem} - l \cdot F_e = 0 \quad (2)$$

Here, ΔG is the total free energy difference per base pair between the extended and condensed states of DNA at the equilibrium; ΔG_{chem} is the DNA−DNA attraction without external force, which includes contributions of electrostatic interactions and bending of DNA; F_e is the equilibrium condensation force (Figure 5e−h); l is the DNA extension per base at F_e, which depends on the elasticity of DNA for the given condition (i.e., methylation status and cation concentration). We calculated l using the extensible worm-like chain model with determined values of P, L, and K (Figure 6).

As shown in Figure 7a−d, we calculated the ΔG_{chem} for C-DNA, mCpG-DNA, and mC-DNA. To determine the effects of cytosine methylation, we further calculated the changes in ΔG_{chem} caused by cytosine methylation ($\Delta\Delta G_{chem}$, Figure 7e−h). We found $\Delta\Delta G_{chem}$ was larger at lower concentrations of high-valent cations. At 0.01 mM $Spermine^{4+}$, $\Delta\Delta G_{chem}$ approaches ~0.04 k_BT/bp for mCpG-DNA (~0.23 k_BT per methylated cytosine nucleotide) and ~0.08 k_BT/bp for mC-DNA (~0.15 k_BT per methylated cytosine nucleotide). At 0.01 mM PLL^{6+}, $\Delta\Delta G_{chem}$ approaches ~0.03 k_BT/bp for mCpG-DNA (~0.18 k_BT per methylated cytosine nucleotide) and ~0.08 k_BT/bp for mC-DNA (~0.14 k_BT per methylated cytosine nucleotide). It appears that cytosine methylation at CpG sites increases DNA−DNA attraction more significantly than cytosine methylation at other sites. As shown in Figure 7i−l, at 0.01 mM $Sperimine^{4+}$, 5mCpG increases ΔG_{chem} by ~32% and 5mC further increases ΔG_{chem} by ~65% for our ~57% GC DNA fragment. At 0.01 mM PLL^{6+}, 5mCpG increases ΔG_{chem} by ~9% and 5mC further increases ΔG_{chem} by ~21%.

■ DISCUSSION

In previous single-molecule DNA condensation experiments, the DNA was directly tethered between the bead and glass surfaces and the decondensation showed step-wise kinetics in a

https://dx.doi.org/10.1021/jacs.9b11957
J. Am. Chem. Soc. 2020, 142, 9203−9209

wide range of applied force. The complete decondensation cannot be accomplished even at the force of 23 pN in the presence of $CoHex^{3+}$.[18] By using long dsRNA handles to protect the inside dsDNA from DNA−surface interactions, we observed the hopping kinetics between the condensed and extended states of DNA at constant forces at the equilibrium (Figure 4). Forces of ∼0.2 pN higher than the equilibrium force lead to complete decondensation of the DNA (Figure 4). The equilibrium condensation force depends on the concentration of high-valent cations and achieves a maximum of ∼3.2 pN for $CoHex^{3+}$, ∼0.9 pN for $Spermidine^{3+}$, and ∼4.0 pN for $Spermine^{4+}$ using C-DNA. Using the RNA−DNA−RNA structure, our nucleation force achieves a maximum of ∼0.8 pN for $CoHex^{3+}$, ∼0.3 pN for $Spermidine^{3+}$, and ∼0.9 pN for $Spermine^{4+}$ using C-DNA, which are far below the previous values obtained from the directly tethered DNA molecules for the same high-valent cations.[13,15−18] Thus, if DNA was directly tethered to the surfaces, the DNA−surface interactions might disturb the DNA condensation experiments.

Biological regulations often operate at margin zones of phase transition. The enhancement of DNA−DNA attraction caused by CpG methylation may make a deterministic contribution to DNA condensation under certain conditions, especially when the concentrations of high-valent cations are close to the threshold for DNA condensation. Using $\Delta\Delta G_{chem}$ of 0.03 k_BT/bp and considering that the perimeter of the toroids is 100−300 nm (about 300−1000 bp), 5mCpG increases the DNA−DNA attraction by about 9−30 k_BT for each circle in the toroids. This increase in DNA−DNA attraction caused by 5mCpG is strong enough to suppress the thermal energy, which should make a valid contribution to DNA condensation. The enhancement of G_{chem} by CpG methylation may explain why sperm DNA has the highest level of CpG methylation from the thermodynamic perspective. Recall that PLL^{6+} serves as a reduced model of histone tails that modulate nucleosome organizations and interactions. In the presence of PLL^{6+}, methylation of each cytosine nucleotide at CpG sites increases ΔG_{chem} by up to ∼0.18 k_BT, which may be related to the role of 5mCpG in the subtle regulation of nucleosome stability revealed in previous experiments.[34−39]

It is reasonable that cytosine methylation increases the DNA−DNA attraction in the presence of high-valent cations. As revealed in the previous simulations, cytosine methylation provides the exclusion-volume effects in grooves for suppressing internal cation-binding deeply in grooves and correspondingly increases the external cation-binding around phosphate groups.[19] Such stronger external cation-binding would favor the high-valent cation-bridging effect between DNA chains and increase DNA−DNA attraction.[19,40−42] As cytosine methylation mostly had no detectable effects on the elasticity of DNA in the presence of high-valent cations (Figure 6), likely the enhancement in G_{chem} are dominatingly caused by changes in electrostatic interactions.

In addition to DNA condensation, our measurements may also help to evaluate the effects of cytosine methylation on other processes of DNA, including bundling, crystallization, looping, supercoiling, bridging, cross-linking, crossing over, juxtaposition, knotting, and entanglement, where direct DNA−DNA contacts are involved. DNA−DNA contacts are involved in many fundamental biological processes such as homological recombination,[43] DNA packaging and ejection of virals,[32] chromatin dynamics and remodeling,[44] formation of heterochromatin at highly CpG-methylated DNA,[45] trans-silencing increased with DNA methylation,[46] promoter-enhancer interactions for transcription regulation.[47] DNA−DNA contacts are also involved in many applications such as DNA origami/nanostructures,[48] gene delivery and gene therapy,[49] DNA-guided organic semiconductor,[50] DNA aptamers and sensors.[51] For example, since cytosine methylation enhances DNA condensation, the cytosine-methylated DNA might be a better "genetic cargo" in cationic liposome- or polymer-based gene delivery systems.

Recent simulations revealed that external binding of high-valent cations around phosphate groups softened DNA while the internal binding of high-valent cations deeply in grooves could counteract the above affect.[27,52] It is understandable that cytosine methylation slightly softens DNA in the presence of $CoHex^{3+}$ but has no detectable effect on the DNA stiffness in the presence of $Spermine^{4+}$ (Figure 6a,c). The increase of external cation-binding and the decreased internal cation-binding caused by the exclusion effect of cytosine methylation would slightly soften the DNA in the presence of $CoHex^{3+}$. As indicated in recent simulations, compared with $CoHex^{3+}$, $Spermine^{4+}$ has a slightly stronger tendency for external binding around phosphate groups and slightly less tendency for internal binding in grooves.[29] Thus, the exclusion effect in grooves from cytosine methylation would be slightly stronger for the binding of $CoHex^{3+}$ than for that of $Spermine^{4+}$, and resultantly, cytosine methylation can slightly soften the DNA in the presence of $CoHex^{3+}$ while not in the presence of $Spermine^{4+}$.

Controversial results about the effects of cytosine methylation on the stiffness of DNA were obtained in experiments and simulations previously. Single-molecule cyclization experiments revealed that cytosine methylation stiffened DNA.[37−39] Nevertheless, optical/magnetic tweezing and AFM scanning experiments revealed that cytosine methylation softened DNA.[53,54] Previous simulations reported varied results also: cytosine methylation either stiffened DNA[37−39,55,56] or had no effect[57] or softened DNA.[58,59] A part of the contradicting results is probably due to the concept of flexibility, which in reality depends on the nature of the distortion. Another part is probably related to the technique used and the type of observable collected. In this work, we found cytosine methylation slightly softened DNA in the presence of $CoHex^{3+}$, while it mostly had no detectable effects on the stiffness of DNA. Thus, the effects of cytosine methylation on DNA stiffness might be sensitive to conditions such as cations, GC content, DNA length, and local sequence pattern, which calls for future systematic studies.

■ ASSOCIATED CONTENT

Supporting Information

The Supporting Information is available free of charge at https://pubs.acs.org/doi/10.1021/jacs.9b11957.

Figures S1−S4 (PDF)

■ AUTHOR INFORMATION

Corresponding Author

Xing-Hua Zhang − *College of Life Sciences, the Institute for Advanced Studies, State Key Laboratory of Virology, Hubei Key Laboratory of Cell Homeostasis, Wuhan University, Wuhan 430072, China;* orcid.org/0000-0002-9487-191X; Phone: +86-27-68755477; Email: zhxh@whu.edu.cn; Fax: +86-27-68752560

https://dx.doi.org/10.1021/jacs.9b11957
J. Am. Chem. Soc. 2020, 142, 9203−9209

Authors

Ya-Jun Yang − *College of Life Sciences, the Institute for Advanced Studies, State Key Laboratory of Virology, Hubei Key Laboratory of Cell Homeostasis, Wuhan University, Wuhan 430072, China*

Hai-Long Dong − *Department of Physics and Key Laboratory of Artificial Micro & Nano-structures of Ministry of Education, School of Physics and Technology, Wuhan University, Wuhan 430072, China*

Xiao-Wei Qiang − *Department of Physics and Key Laboratory of Artificial Micro & Nano-structures of Ministry of Education, School of Physics and Technology, Wuhan University, Wuhan 430072, China*

Hang Fu − *College of Life Sciences, the Institute for Advanced Studies, State Key Laboratory of Virology, Hubei Key Laboratory of Cell Homeostasis, Wuhan University, Wuhan 430072, China*

Er-Chi Zhou − *College of Life Sciences, the Institute for Advanced Studies, State Key Laboratory of Virology, Hubei Key Laboratory of Cell Homeostasis, Wuhan University, Wuhan 430072, China*

Chen Zhang − *College of Life Sciences, the Institute for Advanced Studies, State Key Laboratory of Virology, Hubei Key Laboratory of Cell Homeostasis, Wuhan University, Wuhan 430072, China*

Lei Yin − *College of Life Sciences, the Institute for Advanced Studies, State Key Laboratory of Virology, Hubei Key Laboratory of Cell Homeostasis, Wuhan University, Wuhan 430072, China*

Xue-Feng Chen − *College of Life Sciences, the Institute for Advanced Studies, State Key Laboratory of Virology, Hubei Key Laboratory of Cell Homeostasis, Wuhan University, Wuhan 430072, China*

Fu-Chao Jia − *Laboratory of Functional Molecules and Materials, School of Physics and Optoelectronic Engineering, Shandong University of Technology, Zibo 255000, China;* orcid.org/0000-0003-1920-6888

Liang Dai − *Department of Physics, City University of Hong Kong, Hong Kong 999077, China;* orcid.org/0000-0002-4672-6283

Zhi-Jie Tan − *Department of Physics and Key Laboratory of Artificial Micro & Nano-structures of Ministry of Education, School of Physics and Technology, Wuhan University, Wuhan 430072, China*

Complete contact information is available at: https://pubs.acs.org/10.1021/jacs.9b11957

Notes

The authors declare no competing financial interest.

■ ACKNOWLEDGMENTS

This work was supported by the National Natural Science Foundation of China [31670760, 11704286, and 11774272].

■ REFERENCES

(1) Conwell, C. C.; Vilfan, I. D.; Hud, N. V. Controlling the size of nanoscale toroidal DNA condensates with static curvature and ionic strength. *Proc. Natl. Acad. Sci. U. S. A.* **2003**, *100*, 9296−301.

(2) Bloomfield, V. A. DNA condensation. *Curr. Opin. Struct. Biol.* **1996**, *6*, 334−41.

(3) Jones, P. A. Functions of DNA methylation: islands, start sites, gene bodies and beyond. *Nat. Rev. Genet.* **2012**, *13*, 484−92.

(4) Smith, Z. D.; Meissner, A. DNA methylation: roles in mammalian development. *Nat. Rev. Genet.* **2013**, *14*, 204−20.

(5) Bergman, Y.; Cedar, H. DNA methylation dynamics in health and disease. *Nat. Struct. Mol. Biol.* **2013**, *20*, 274−81.

(6) Li, E.; Zhang, Y. DNA Methylation in Mammals. *Cold Spring Harbor Perspect. Biol.* **2014**, *6*, a019133.

(7) Melnikov, S. M.; Sergeyev, V. G.; Yoshikawa, K. Transition of Double-Stranded DNA Chains between Random Coil and Compact Globule States Induced by Cooperative Binding of Cationic Surfactant. *J. Am. Chem. Soc.* **1995**, *117*, 9951−9956.

(8) Brewer, L. R.; Corzett, M.; Balhorn, R. Protamine-induced condensation and decondensation of the same DNA molecule. *Science* **1999**, *286*, 120−3.

(9) Husale, S.; Grange, W.; Karle, M.; Burgi, S.; Hegner, M. Interaction of cationic surfactants with DNA: a single-molecule study. *Nucleic Acids Res.* **2008**, *36*, 1443−9.

(10) Wang, X. L.; Zhang, X. H.; Cao, M. W.; Zheng, H. Z.; Xiao, B.; Wang, Y. L.; Li, M. Gemini Surfactant-Induced DNA Condensation into a Beadlike Structure. *J. Phys. Chem. B* **2009**, *113*, 2328−32.

(11) Ritort, F.; Mihardja, S.; Smith, S. B.; Bustamante, C. Condensation transition in DNA-polyaminoamide dendrimer fibers studied using optical tweezers. *Phys. Rev. Lett.* **2006**, *96*, 118301.

(12) Dobrynin, A. V. Effect of counterion condensation on rigidity of semiflexible polyelectrolytes. *Macromolecules* **2006**, *39*, 9519−27.

(13) Todd, B. A.; Parsegian, V. A.; Shirahata, A.; Thomas, T. J.; Rau, D. C. Attractive forces between cation condensed DNA double helices. *Biophys. J.* **2008**, *94*, 4775−4782.

(14) Baumann, C. G.; Bloomfield, V. A.; Smith, S. B.; Bustamante, C.; Wang, M. D.; Block, S. M. Stretching of single collapsed DNA molecules. *Biophys. J.* **2000**, *78*, 1965−78.

(15) Besteman, K.; Hage, S.; Dekker, N. H.; Lemay, S. G. Role of tension and twist in single-molecule DNA condensation. *Phys. Rev. Lett.* **2007**, *98*, No. 058103.

(16) Besteman, K.; Van Eijk, K.; Lemay, S. G. Charge inversion accompanies DNA condensation by multivalent ions. *Nat. Phys.* **2007**, *3*, 641−4.

(17) Li, W.; Wong, W. J.; Lim, C. J.; Ju, H. P.; Li, M.; Yan, J.; Wang, P. Y. Complex kinetics of DNA condensation revealed through DNA twist tracing. *Phys. Rev. E* **2015**, *92*, No. 022707.

(18) Fu, W. B.; Wang, X. L.; Zhang, X. H.; Ran, S. Y.; Yan, J.; Li, M. Compaction dynamics of single DNA molecules under tension. *J. Am. Chem. Soc.* **2006**, *128*, 15040−1.

(19) Yoo, J.; Kim, H.; Aksimentiev, A.; Ha, T. Direct evidence for sequence-dependent attraction between double-stranded DNA controlled by methylation. *Nat. Commun.* **2016**, *7*, 11045.

(20) Kang, H.; Yoo, J.; Sohn, B. K.; Lee, S. W.; Lee, H. S.; Ma, W.; Kee, J. M.; Aksimentiev, A.; Kim, H. Sequence-dependent DNA condensation as a driving force of DNA phase separation. *Nucleic Acids Res.* **2018**, *46*, 9401−13.

(21) Zhao, X. C.; Fu, H.; Song, L.; Yang, Y. J.; Zhou, E. C.; Liu, G. X.; Chen, X. F.; Li, Z.; Wu, W. Q.; Zhang, X. H. S-DNA and RecA/RAD51-Mediated Strand Exchange in Vitro. *Biochemistry* **2019**, *58*, 2009−16.

(22) Zhang, C.; Fu, H.; Yang, Y. J.; Zhou, E. C.; Tan, Z. J.; You, H. J.; Zhang, X. H. The Mechanical Properties of RNA-DNA Hybrid Duplex Stretched by Magnetic Tweezers. *Biophys. J.* **2019**, *116*, 196−204.

(23) Yang, Y. J.; Song, L.; Zhao, X. C.; Zhang, C.; Wu, W. Q.; You, H. J.; Fu, H.; Zhou, E. C.; Zhang, X. H. A Universal Assay for Making DNA, RNA, and RNA-DNA Hybrid Configurations for Single-Molecule Manipulation in Two or Three Steps without Ligation. *ACS Synth. Biol.* **2019**, *8*, 1663−72.

(24) Zhang, X. H.; Qu, Y. Y.; Chen, H.; Rouzina, I.; Zhang, S. L.; Doyle, P. S.; Yan, J. Interconversion between three overstretched DNA structures. *J. Am. Chem. Soc.* **2014**, *136*, 16073−80.

(25) Zhang, X. H.; Chen, H.; Le, S. M.; Rouzina, I.; Doyle, P. S.; Yan, J. Revealing the competition between peeled ssDNA, melting bubbles, and S-DNA during DNA overstretching by single-molecule calorimetry. *Proc. Natl. Acad. Sci. U. S. A.* **2013**, *110*, 3865−70.

(26) Zhang, X. H.; Chen, H.; Fu, H. X.; Doyle, P. S.; Yan, J. Two distinct overstretched DNA structures revealed by single-molecule thermodynamics measurements. *Proc. Natl. Acad. Sci. U. S. A.* **2012**, *109*, 8103−8.
(27) Fu, H.; Zhang, C.; Qiang, X. W.; Yang, Y. J.; Dai, L.; Tan, Z. J.; Zhang, X. H. Opposite Effects of High-Valent Cations on the Elasticities of DNA and RNA Duplexes Revealed by Magnetic Tweezers. *Phys. Rev. Lett.* **2020**, *124*, No. 058101.
(28) Li, L.; Pabit, S. A.; Meisburger, S. P.; Pollack, L. Double-stranded RNA resists condensation. *Phys. Rev. Lett.* **2011**, *106*, 108101.
(29) Kuzmanic, A.; Dans, P. D.; Orozco, M. An In-Depth Look at DNA Crystals through the Prism of Molecular Dynamics Simulations. *Chem-Us* **2019**, *5*, 649−63.
(30) Qiu, X.; Rau, D. C.; Parsegian, V. A.; Fang, L. T.; Knobler, C. M.; Gelbart, W. M. Salt-dependent DNA-DNA spacings in intact bacteriophage lambda reflect relative importance of DNA self-repulsion and bending energies. *Phys. Rev. Lett.* **2011**, *106*, No. 028102.
(31) Yoo, J.; Aksimentiev, A. The structure and intermolecular forces of DNA condensates. *Nucleic Acids Res.* **2016**, *44*, 2036−46.
(32) Keller, N.; delToro, D.; Grimes, S.; Jardine, P. J.; Smith, D. E. Repulsive DNA-DNA interactions accelerate viral DNA packaging in phage Phi29. *Phys. Rev. Lett.* **2014**, *112*, 248101.
(33) Odijk, T. Stiff Chains and Filaments under Tension. *Macromolecules* **1995**, *28*, 7016−8.
(34) Choy, J. S.; Wei, S.; Lee, J. Y.; Tan, S.; Chu, S.; Lee, T. H. DNA Methylation Increases Nucleosome Compaction and Rigidity. *J. Am. Chem. Soc.* **2010**, *132*, 1782−3.
(35) Lee, J. Y.; Lee, J.; Yue, H.; Lee, T. H. Dynamics of Nucleosome Assembly and Effects of DNA Methylation. *J. Biol. Chem.* **2015**, *290*, 4291−303.
(36) Lee, J. Y.; Lee, T. H. Effects of DNA Methylation on the Structure of Nucleosomes. *J. Am. Chem. Soc.* **2012**, *134*, 173−5.
(37) Perez, A.; Castellazzi, C. L.; Battistini, F.; Collinet, K.; Flores, O.; Deniz, O.; Ruiz, M. L.; Torrents, D.; Eritja, R.; Soler-Lopez, M.; Orozco, M. Impact of Methylation on the Physical Properties of DNA. *Biophys. J.* **2012**, *102*, 2140−8.
(38) Ngo, T. T. M.; Yoo, J.; Dai, Q.; Zhang, Q.; He, C.; Aksimentiev, A.; Ha, T. Effects of cytosine modifications on DNA flexibility and nucleosome mechanical stability. *Nat. Commun.* **2016**, *7*, 10813.
(39) Nathan, D.; Crothers, D. M. Bending and flexibility of methylated and unmethylated EcoRI DNA. *J. Mol. Biol.* **2002**, *316*, 7−17.
(40) Tolokh, I. S.; Pabit, S. A.; Katz, A. M.; Chen, Y.; Drozdetski, A.; Baker, N.; Pollack, L.; Onufriev, A. V. Why double-stranded RNA resists condensation. *Nucleic Acids Res.* **2014**, *42*, 10823−31.
(41) Wu, Y. Y.; Zhang, Z. L.; Zhang, J. S.; Zhu, X. L.; Tan, Z. J. Multivalent ion-mediated nucleic acid helix-helix interactions: RNA versus DNA. *Nucleic Acids Res.* **2015**, *43*, 6156−65.
(42) Katz, A. M.; Tolokh, I. S.; Pabit, S. A.; Baker, N.; Onufriev, A. V.; Pollack, L. Spermine Condenses DNA, but Not RNA Duplexes. *Biophys. J.* **2017**, *112*, 22−30.
(43) Lee, C. Y.; Su, G. C.; Huang, W. Y.; Ko, M. Y.; Yeh, H. Y.; Chang, G. D.; Lin, S. J.; Chi, P. Promotion of homology-directed DNA repair by polyamines. *Nat. Commun.* **2019**, *10*, 65.
(44) Risca, V. I.; Denny, S. K.; Straight, A. F.; Greenleaf, W. J. Variable chromatin structure revealed by in situ spatially correlated DNA cleavage mapping. *Nature* **2017**, *541*, 237−41.
(45) Strom, A. R.; Emelyanov, A. V.; Mir, M.; Fyodorov, D. V.; Darzacq, X.; Karpen, G. H. Phase separation drives heterochromatin domain formation. *Nature* **2017**, *547*, 241−5.
(46) Muskens, M. W.; Vissers, A. P.; Mol, J. N.; Kooter, J. M. Role of inverted DNA repeats in transcriptional and post-transcriptional gene silencing. *Plant Mol. Biol.* **2000**, *43*, 243−60.
(47) Ron, G.; Globerson, Y.; Moran, D.; Kaplan, T. Promoter-enhancer interactions identified from Hi-C data using probabilistic models and hierarchical topological domains. *Nat. Commun.* **2017**, *8*, 2237.
(48) Pinheiro, A. V.; Han, D.; Shih, W. M.; Yan, H. Challenges and opportunities for structural DNA nanotechnology. *Nat. Nanotechnol.* **2011**, *6*, 763−72.
(49) El-Aneed, A. An overview of current delivery systems in cancer gene therapy. *J. Controlled Release* **2004**, *94*, 1−14.
(50) Back, S. H.; Park, J. H.; Cui, C.; Ahn, D. J. Bio-recognitive photonics of a DNA-guided organic semiconductor. *Nat. Commun.* **2016**, *7*, 10234.
(51) Liu, J.; Cao, Z.; Lu, Y. Functional nucleic acid sensors. *Chem. Rev.* **2009**, *109*, 1948−98.
(52) Drozdetski, A. V.; Tolokh, I. S.; Pollack, L.; Baker, N.; Onufriev, A. V. Opposing Effects of Multivalent Ions on the Flexibility of DNA and RNA. *Phys. Rev. Lett.* **2016**, *117*, No. 028101.
(53) Pongor, C. I.; Bianco, P.; Ferenczy, G.; Kellermayer, R.; Kellermayer, M. Optical Trapping Nanometry of Hypermethylated CPG-Island DNA. *Biophys. J.* **2017**, *112*, 512−22.
(54) Shon, M. J.; Rah, S. H.; Yoon, T. Y. Submicrometer elasticity of double-stranded DNA revealed by precision force-extension measurements with magnetic tweezers. *Sci. Adv.* **2019**, *5*, eaav1697.
(55) Derreumaux, S.; Chaoui, M.; Tevanian, G.; Fermandjian, S. Impact of CpG methylation on structure, dynamics and solvation of cAMP DNA responsive element. *Nucleic Acids Res.* **2001**, *29*, 2314−26.
(56) Temiz, N. A.; Donohue, D. E.; Bacolla, A.; Luke, B. T.; Collins, J. R. The Role of Methylation in the Intrinsic Dynamics of B- and Z-DNA. *PLoS One* **2012**, *7*, No. e35558.
(57) Karolak, A.; van der Vaart, A. Enhanced Sampling Simulations of DNA Step Parameters. *J. Comput. Chem.* **2014**, *35*, 2297−304.
(58) Liebl, K.; Zacharias, M. How methyl-sugar interactions determine DNA structure and flexibility. *Nucleic Acids Res.* **2019**, *47*, 1132−40.
(59) Carvalho, A. T. P.; Gouveia, L.; Kanna, C. R.; Warmlander, S. K. T. S.; Platts, J. A.; Kamerlin, S. C. L. Understanding the structural and dynamic consequences of DNA epigenetic modifications: Computational insights into cytosine methylation and hydroxymethylation. *Epigenetics* **2014**, *9*, 1604−12.

https://dx.doi.org/10.1021/jacs.9b11957
J. Am. Chem. Soc. 2020, 142, 9203−9209